Design of Super-Twisting Sliding Mode Observer for LISA Mission Micro-Meteoroid Impact

Design of Super-Twisting Sliding Mode Observer for LISA Mission Micro-Meteoroid Impact

D. Ruggiero[1], E. Capello[2], C. Novara[3] and J. Grzymisch[4]

***Abstract*— LISA (Laser Interferometer Space Antenna) is a space mission, under study by the European Space Agency (ESA) and other institutions, with the objective of detecting, observing, and measuring gravitational waves. It consists of a triangle constellation of three spacecraft connected through bi-directional laser links to measure gravitational waves by means of interferometry. During the Science mode, also called Drag-free mode, micrometeoroids may collide with the spacecraft surface, generating impulsive forces and torques, which can cause the loss of links. Impulsive disturbances may lead to a significant performance degradation and even to instability, especially in the presence of actuator saturations. In this paper, a Navigation algorithm based on a sliding mode observer is proposed to improve the closed-loop system stability properties, allowing the spacecraft to quickly restore the laser links, safely returning to the Science mode. Simulation results show the effectiveness of the proposed solution. Moreover, a comparison with classical methods is carried out, based on the combination of an Extended Kalman Filter and an Anti-windup strategy.**

I. Introduction

LISA is a space mission, currently under study by ESA, for the detection and measurement of gravitational waves. It consists of three spacecraft describing a triangular constellation of 2.5 Mkm side-length, where each spacecraft is connected to the others through bi-directional laser beams. All the details about how the triangular configuration is reached and about each LISA mission phase are provided in [1], [2]. Anyhow, when the constellation of the three spacecraft is acquired, the main objective of the mission is to measure through laser beams the relative position of two far cubic test masses (TMs) placed in two different spacecraft, and to detect gravitational waves by means of laser interferometry. To perform the desired measurements, the TMs must have free-fall condition, with the spacecraft compensating for external disturbances and sensors noise, so that each TM position and attitude fulfils tight requirements at nanoscopic scale. Consequentially, a drag-free control system has been designed in [3], [4], in order to keep the laser links and to perform small adjustments around the working point compensating for external disturbances. However, as observed during the LISA Pathfinder mission [5], [6], the Science mode can be affected by micro-meteorite impacts, leading to high perturbation in spacecraft attitude and TMs position. The micro-meteorite impact phenomena has been already studied in [7], in which the results show that some impacts have sufficient energy to cause a perturbation in the spacecraft attitude, with an unstable behaviour. As known from literature [8], input nonlinearities may lead to performance degradation and even instability, especially in presence of actuator saturation. For the LISA spacecraft, the attitude closed-loop system is subject to nonlinearities, mainly due to impulsive disturbance and measurement noise. Laser links are, in fact, the main source of high precision attitude measurements. High perturbations imply links loss, and the need to use a different sensor to measure the spacecraft attitude, generally characterized by lower precision and higher noise.

The main purpose of this work is to propose an effective strategy to recover the laser links and restoring the constellation. An observer-based navigation algorithm, based on super-twisting sliding mode technique [9], [10] is designed to improve the spacecraft attitude closed-loop stability, handling different sensors. The closed-loop performance in terms of attitude stabilization and laser links recovery time are evaluated and compared in simulation with an Anti-windup strategy combined with an Extended Kalman filter (EKF). This combination is a typical solution to improve closed-loop performance under actuator saturation [11], [12], [13]. Since one of the purpose of this research is to design an observer as direct interface between sensors and controller, several observer strategies are analyzed, such as Luenberger observer [14], [15], Kalman filter [16], Extended Kalman filter (EKF) [17], and first-order sliding mode observer [18]. However, these alternative strategies cannot improve the stability properties of the the closed-loop system or do not provide the needed accuracy for laser link re-acquisition. Thus, the novelty of this study consists in the implementation of super-twisting sliding mode observer as a direct interface between sensors and control system, to improve the accuracy and the stability of the proposed closed-loop system. Even if its main applications in literature are as estimator of disturbances and failure, [19], [20], [21], in this work it improves the closed-loop stability in presence of nonlinearities (for example the micro-meteorite impact and the laser links loss) and, combined with a feedback control system,

This work is part of the LISA DFACS preliminary prototyping study under the European Space Agency Technology Development Element program.

[1] D. Ruggiero is with the Department of Mechanical and Aerospace Engineering, Politecnico di Torino, Turin, 10129, Italy. dario.ruggiero@polito.it

[2] E. Capello is with the Department of Mechanical and Aerospace Engineering, Politecnico di Torino, and with the CNR-IEIIT, Politecnico di Torino, Corso Duca degli Abruzzi 24, 10129 Torino, Italy. elisa.capello@polito.it

[3] C. Novara is with the Department of Electronics and Telecommunications, Politecnico di Torino, Turin, 10129, Italy. carlo.novara@polito.it

[4] J. Grzymisch is with the Guidance, Navigation and Control Section (TEC-SAG), ESTEC, European Space Agency, Kepleralaan 1, Noordwijk 2201 AZ, The Netherlands. Jonathan.Grzymisch@esa.int

it is able to stabilize the spacecraft, restoring autonomously the laser links. The EKF solution combined with an anti-windup approach is considered as noise filtering technique, in comparison with the proposed observer strategy.

The paper is organized as follow. In Sec.I the nonlinear model of the LISA spacecraft is presented, and data about sensors and actuators are provided to fully understand the problem. The sliding mode observer design is reported in Sec.III. Simulations results are provided in Sec.IV and, finally, conclusion are given in Sec.V. The Anti-windup strategy and EKF are described in the Appendix.

II. Nonlinear Mathematical Model

In this section, the LISA spacecraft nonlinear simulator used to evaluate the considered navigation algorithms is described. More details about the model and its validation can be found in [22]. In this paper, only the dynamics related to the attitude stabilization is detailed, including actuator and sensor systems. Note that in the LISA mission the complete system includes the TMs, three spacecraft in triangular formation and optical assemblies, which are out of the scope of this paper. The main focus is Science mode, where the laser links are active and the overall system is regulated by a decoupled drag-free control system, which consists in 16 Single-Input Single-Output (SISO) Linear time-invariant (LTI) systems working at 10 Hz, and obtained with the mixed-sensitivity H_∞ procedure. More details can be found in [4]. The main attitude sensor employed during this mission phase is the Differential Wavefront Sensor (DWS) that uses the laser links to measure the spacecraft attitude in the constellation reference frame (CRF) with a nanometric precision. The proposed strategy, as said in the Introduction, is considered when a micro-meteorite impacts the spacecraft. This impact affects the attitude stability and may be critical, if the laser links is lost. We can define the following reference frames. The CRF is built on board to evaluate the attitude with respect to the constellation formation. It is centered in the spacecraft and defined by the set $\{O_C, \mathbf{c}_1, \mathbf{c}_2, \mathbf{c}_3\}$, with $\mathbf{c}_1$ lying in the plane containing the two laser links and defined as the bisector of the angle between the links, $\mathbf{c}_3$ perpendicular to the plane, and $\mathbf{c}_2$ is chosen according to the right-handed coordinate system.

The inertial reference frame (IRF) is a quasi-inertial reference frame centered in the Sun and defined by the set $\{O_I, \mathbf{I}_1, \mathbf{I}_2, \mathbf{I}_3\}$, with $\mathbf{I}_1$ directed along the the line connecting Sun and Earth at Vernal Equinox, $\mathbf{I}_3$ is perpendicular to Earth's orbital plane around the sun, and $\mathbf{I}_2$ is chosen according to the right-handed coordinate system.

Finally, the spacecraft reference frame (SRF) is the traditional reference frame fixed with the spacecraft's body and defined by the set $\{O_S, \mathbf{s}_1, \mathbf{s}_2, \mathbf{s}_3\}$. In nominal conditions SRF overlaps CRF. Reference frames are rapresented in Figure 1.

TABLE I

Attitude sensors: noise and range order of magnitude.

Sensor	Range	Noise σ	Working frequency (Hz)
DWS	μrad	nrad	100
CAS	mrad	μrad	10
STR θ_1	rad	μrad	5
STR θ_2	rad	μrad	5
STR θ_3	rad	10 μrad	5

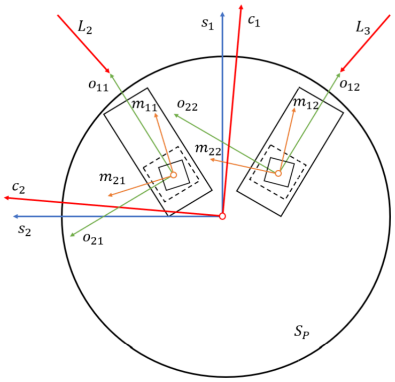

Fig. 1. Reference frames [22]

When the link is lost, the Constellation Acquisition Sensor (CAS) measures the attitude in the CRF frame. However, this sensor is less accurate with respect to DWS, but its range is higher. In same critical situations, the spacecraft could be out of CAS range and only the Star Tracker (STR) can be employed, first to recover the CAS, and finally the laser links and the DWS. Compared with the other two sensors, the STR provides measurements of the spacecraft attitude in the (IRF) with a different and lower precision for each degree-of-freedom. Some data of the sensors are in Table I.

The attitude dynamics is described in the SRF as follows. The angular velocity of the spacecraft with respect to the constellation is simply defined by

$$\omega_{SC}^S = \omega_{SI}^S - T_C^S \omega_{CI}^C, \tag{1}$$

where $\omega_{SI}^S \in \mathbb{R}^3$ is the angular velocity of the spacecraft, $\omega_{CI}^C \in \mathbb{R}^3$ is the angular velocity of the constellation measured in CRF, and $T_C^S \in \mathbb{R}^{3\times3}$ is the coordinate transformation matrix from CRF to SRF. The attitude dynamics equation is computed as the time derivative of Equation (1), as

$$\dot{\omega}_{SC}^S = \dot{\omega}_{SI}^S - T_C^S \dot{\omega}_{CI}^C + \omega_{SC}^S \times T_C^S \omega_{CI}^C, \tag{2}$$

where $\omega_{CI}^C, \dot{\omega}_{CI}^C$ depend on the direction of the incoming laser links, and in general by the spacecraft position in the LISA orbit, while $\dot{\omega}_{SI}^S$ is derived by the angular momentum conservation as

$$\dot{\omega}_{SI}^S = J_S^{-1}\left[-\omega_{SI}^S \times J_S \omega_{SI}^S + M_T^S + D_S^S + M_{met}^S + D_{int}\right], \tag{3}$$

where $J_S \in \mathbb{R}^{3\times3}$ is the spacecraft inertia matrix, $M_T^S \in \mathbb{R}^3$ is the torque provided by the thrusters, and given in the SRF, $D_S^S \in \mathbb{R}^3$ is the torque from the solar pressure, $D_{met}^S \in \mathbb{R}^3$ is the torque generated by the micro-meteorite impact, and, finally, $D_{int} \in \mathbb{R}^3$ is related to OAs and TMs dynamics and control. The torque M_T^S is applied on the spacecraft by micro-propulsion system. A simplified actuator model is

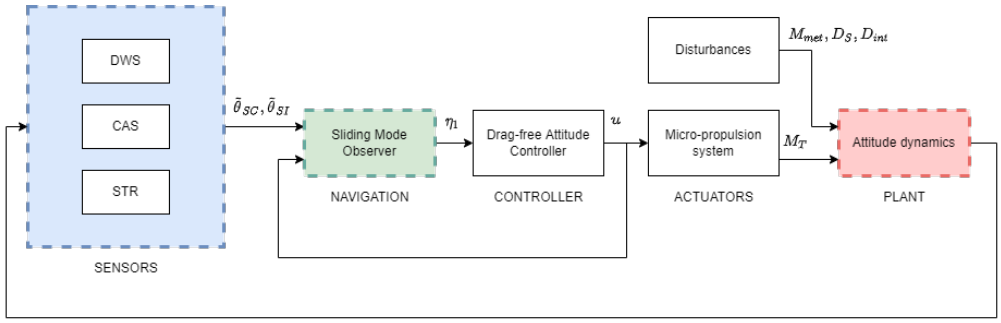

Fig. 2. LISA spacecraft attitude nonlinear model.

considered, to decouple each degree of freedom, as a first order filter with a maximum control authority of 500 μNm and white noise with 0.5 noise power. So, the change of the torque is not instantaneous but requires some seconds with a smooth behavior. The attitude nonlinear model is in Figure 2.

III. Sliding Mode Observer

In this section, the sliding mode observer design is presented. This observer, based on the super-twisting approach, has been developed as a navigation algorithm for the recovery maneuver, when the attitude error is higher than the operative range of the DWS. The main structure of the observer is based on a sliding mode super-twisting approach, and given by

$$\begin{cases} \dot{\eta}_1 = \eta_2 + k_1 |y - \eta_1|^{0.5} \text{sign}(y - \eta_1) \\ \dot{\eta}_2 = \hat{f}(u, \eta_1, \eta_2) + k_2 \text{sign}(y - \eta_1) \end{cases} , \tag{4}$$

where $\hat{f}$ is the nonlinear plant model, and $y - \eta_1$ is the estimation error of the observed variable. The stability and convergence properties of the super-twisting approach are studied and discussed in [23], [24]. In this application, the observed variable y is θ_{SC}, i.e., the spacecraft attitude in CRF frame. The function $\hat{f}$ is given by

$$\hat{f} = J_S^{-1} \left(u - \hat{\omega}_{SC} \times J_S \hat{\omega}_{SC} \right) , \tag{5}$$

where $u \in \mathbb{R}^3$ is the control input saturated according to the actuation authority, $J_S \in \mathbb{R}^{3x3}$ is the spacecraft inertia matrix, and $\hat{\omega}_{SC} \in \mathbb{R}^3$ is the spacecraft angular velocity in CRF frame, and estimated by means of the observer as η_2. Finally, the observer is given by

$$\begin{cases} \dot{\eta}_1 = \eta_2 + k_1 |e_1|^{0.5} \text{sign}(e_1) \\ \dot{\eta}_2 = J_S^{-1} (u - \eta_2 \times J \eta_2) + k_2 \text{sign}(e_1) \end{cases} , \tag{6}$$

where $e_1 = \tilde{\theta}_{SC} - \eta_1 \in \mathbb{R}^3$ is the estimation error, $\tilde{\theta}_{SC} \in \mathbb{R}^3$ is observed variable by the more accurate (available) sensor and $k_i > 0 \in \mathbb{R}$ are constant gains. The signum function affects the estimation precision, which is limited by the constant gains. To fulfill the precision requirements for the mission, the attitude controller is providing the required signal, if the attitude error is small and the available measurement is provided by DWS sensor When the laser link is lost, the observer is activated and assumes that CAS and STR are the available sensors and only the most accurate ones is selected, as in Table I. If the selected sensor is the STR, a nominal guidance is considered, to translate the measurements from IRF to CRF frames, as follows

$$\hat{\theta}_{SC_{STR}} = \tilde{\theta}_{SI} - \tilde{\theta}_{SI,0} , \tag{7}$$

where $\tilde{\theta}_{SI,0}$ is the STR measurement when the DWS is lost. The constant gains k_i are selected toward simulation analysis, and in order to fulfill stability and convergence requirements. So, the control system can works in an operative range, even in presence of high perturbation. This solution is a trade-off between closed-loop performance, the estimation accuracy and its stability. It follows an approximate approach of how the proposed solution acts in the laser links recovery maneuver.

If the impact gives an high perturbation in the spacecraft attitude, a perturbation is generated in the observer estimation error. Hence, we have $|\theta_{SC}| >> |\eta_1|$. In this case, the observer dynamics can be rewritten as

$$\begin{cases} \dot{\eta}_1 = \eta_2 + k_1 |\theta_{SC}|^{0.5} \text{sign}(\theta_{SC}) \\ \dot{\eta}_2 = J_S^{-1} (u - \eta_2 \times J \eta_2) + k_2 \text{sign}(\theta_{SC}) \end{cases} . \tag{8}$$

From the controller side, when the DWS is lost, the input is switched from the measured attitude to η_1, and it is given by

$$\eta_1 = \int \eta_2 \, dt + \int k_1 |\theta_{SC}|^{0.5} \text{sign}(\theta_{SC}) \, dt . \tag{9}$$

The first term is related to η_2 variation, as in Equation (8), and the second term is directly related to the attitude measurement. In particular, the attitude measurement acts on the observer dynamics, expressed by $\dot{\eta}_2$, as a disturbance, while the controller works to stabilize it, counteracting the perturbation. If η_1 is the controller input, it is kept small and stable preserving the closed-loop system stability, while the attitude variation is driven back on DWS operative range. When $|\theta_{SC}| \simeq |\eta_1|$, and $e_1 \simeq 0$, the observer dynamics can be rewritten as

$$\begin{cases} \dot{\eta}_1 = \eta_2 \\ \dot{\eta}_2 = J_S^{-1} (u - \eta_2 \times J \eta_2) - k_2 \text{sign}(e_1) \end{cases} . \tag{10}$$

The discontinuous term in $\dot{\eta}_1$ is negligible. This leads to higher estimation accuracy, and the recovery properties of

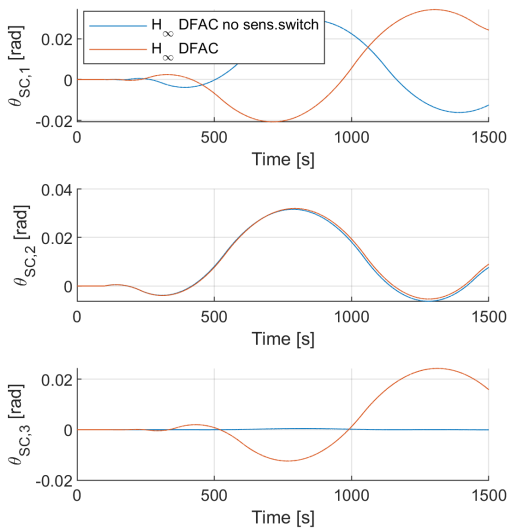

Fig. 3. Strong impact effects during LISA Science mode.

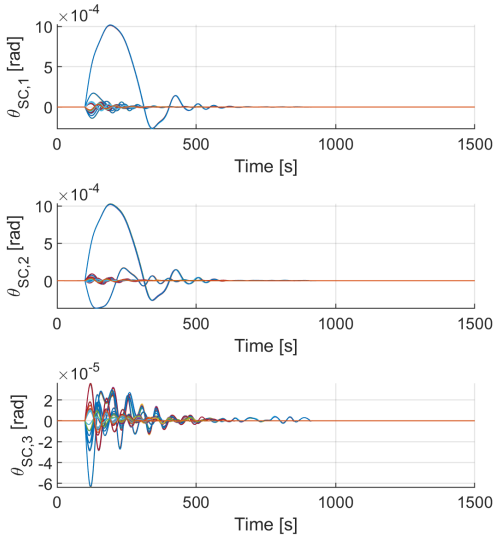

Fig. 5. Attitude time variation in variable impacts simulation campaign.

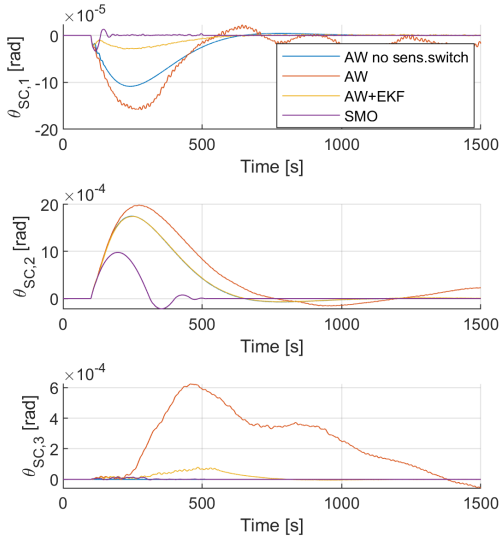

Fig. 4. Comparison between super-twisting sliding mode algorithm and Anti-windup strategy for spacecraft attitude recovery.

the sensor are improved if the real attitude is close to the estimated one.

IV. Simulation Results

In this section, the simulation results provided by the super-twisting sliding mode approach for the LISA spacecraft attitude recovery are shown and compared with the ones given by an EKF/Anti-windup strategy. The EKF and the Anti-windup strategy are described in the Appendix.

To fully understand the performance degradation introduced by the impact, two simulations have been carried out with the LISA drag-free attitude controller (DFAC). First, the sensors uncertainties introduced by laser-link loss are not included. Second, a more realistic scenario is considered, when both CAS and STR are considered as available sensors. In this second case, a switch between the two sensors is introduced in simulation with a delay of $\Delta t = 10$ s. The simulation scenario considers the strongest impact analyzed in [7], which produces a transferred angular momentum of

$$h_m = \begin{bmatrix} -4 & -19.89 & 0.56 \end{bmatrix} 10^{-3} \text{ Nms} . \qquad (11)$$

It is applied as instantaneous impulsive disturbance in the attitude dynamics. In Figure 3, the behaviour of the spacecraft with the DFAC after the micro-meteorite impact is shown. The instabilities introduced by the impact are amplified by the uncertainties introduced by the sensor noise. The instability of $\theta_{SC,3}$ is mainly related to these nonlinearities. This behaviour can be observed even when the Anti-windup strategy is applied to the controller (see Figure 4). However, the performance are improved with an Extended Kalman Filter (EKF), to attenuate the effect of the noise introduced by the sensors. Finally, Figure 4 shows the comparison between the proposed navigation algorithm, based on super-twisting sliding mode observer, and the anti-windup strategy with the EKF. The observer works at a frequency of 100 Hz. The gains k_i of Equation (6) are $k_1 = 0.00025$ and $k_2 = 2 \cdot 10^{-7}$. The sliding mode observer introduces a significant improvement in the recovery performance, both in terms of errors overshoot, and time needed to reacquire the laser links. In particular, after the initial oscillatory behaviour, typical of sliding mode approaches, when the attitude is driven back in proximity of the working point, the observer output is enough reactive to allow quickly laser-links recovery.

The performance of the DFAC with the sliding mode observer have been also verified and evaluated considering strong impacts with different intensity. Figure 5 shows the attitude time variation characterizing each simulation of the simulations campaign. The performance indices have been

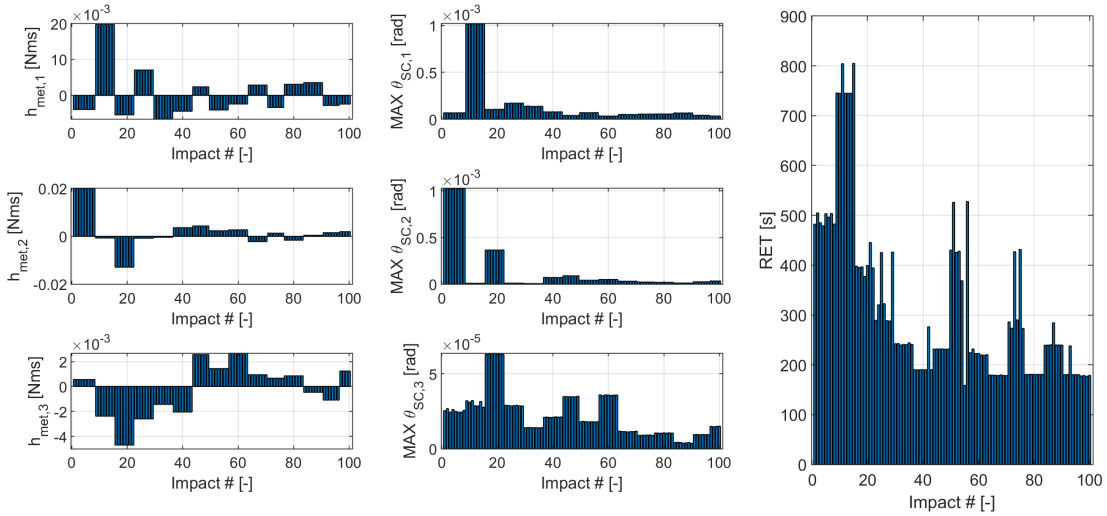

Fig. 6. Exchanged angular momentum and performance indices in variable impacts simulation campaign.

chosen as the maximum overshoot of the attitude error MAX$\theta_{S,i}$ and the time needed to recover the laser links RET. The impact cases, and the values of MAX and RET indices are respectively shown in Figure 6. Also considering impact with similar intensity, the randomness in the sensors noise influence significantly the simulation results. However, the proposed algorithm is able to fulfill the desired tasks for all the considered simulation scenarios.

V. Conclusion

In this paper, the spacecraft attitude stabilization and constellation recovery for the LISA mission is studied, when a micro-meteorite impacts the spacecraft during Science mode. An high intensity impact can produce a perturbation critical for the spacecraft stability. The nonlinearities may become more relevant and the drag-free controller may be not able to handle them anymore. To improve the closed-loop system stability properties, a navigation algorithm, based on super-twisting sliding mode observer, has been developed. The performance of the proposed algorithm has been highlighted by comparing the obtained results with those given by an EKF/Anti-windup approach, and by considering different scenarios. The proposed navigation algorithm improves the stability properties of the closed-loop system, so that the controller is able to recover from the impact, restoring the laser links and the desired attitude in each considered scenario.

APPENDIX

Anti-windup strategy

Due to actuator saturations, the spacecraft attitude controller may not be able to maintain the desired orientation after the spacecraft is hit by a meteoroid. To mitigate this issue, an anti-windup (AW) strategy has been developed.

As discussed above, in this paper we focus on the Science mode of the LISA mission, where the overall system is regulated by a decoupled drag-free control system, consisting of 16 SISO LTI controllers. Let s be the Laplace variable and $K_{DF,i}(s)$ be the SISO controller for the ith spacecraft Euler angle $\theta_{SC,i}$, $i = 1,2,3$. Without AW strategy, the ith attitude control input is

$$u_i = \text{sat}\left(K_{DF,i}(s)\,\theta_{SC,i}\right) \ , \tag{12}$$

where $\text{sat}(\cdot)$ is the saturation function (the saturation bounds are not specified since the strategy described here is general). However, when a strong meteoroid impact occurs, the saturation may not allow $K_{DF,i}(s)$ to properly provide its control action, leading to large attitude oscillations or even to instability.

In order to reduce these issues, an AW strategy has been developed, based on the following controllers:

$$\begin{aligned} C_y(s) &= \frac{N_K(s)}{W(s)} \\ C_u(s) &= 1 - \frac{D_K(s)}{W(s)} \end{aligned},$$

where $N_K(s)$ and $D_K(s)$ are the numerator and denominator of $K_{DF,i}(s)$, respectively, $W(s) = (s/p+1)^{n_K}$, n_K is the order of $K_{DF,i}(s)$ and p is a design parameter.

The control law of the AW strategy for the ith input is

$$u_i = \text{sat}\left(C_y(s)\,\theta_{SC,i} + C_u(s)\,\text{sat}(u_i)\right) \ . \tag{13}$$

It can be easily seen that, without saturation, the AW control input (13) is equivalent to the control input (12). On the other hand, when the saturation is active, the control input (13) takes into account the actual command applied to the plant (given by $\text{sat}(u_i)$) and uses this information to compensate the effects of the saturation.

Extended Kalman filter design

To improve the performance of the anti-windup strategy under high sensor uncertainties, an EKF has been imple-

mented, allowing us to efficiently handle the attitude sensor switch.

The spacecraft attitude model considered in this paper can be written in state space form as

$$\begin{cases} \dot{x} &= A(x)x + Bu + Bd^u \\ y &= Cx + d^y \end{cases}, \tag{14}$$

where the matrices $A \in \mathbb{R}^{6\times6}$, $B \in \mathbb{R}^{6\times3}$ and $C \in \mathbb{R}^{6\times3}$ are obtained from the dynamics and kinematics of the rigid body. The state variable $x \in \mathbb{R}^6$ is defined as the vector $x = \{\theta_{SC}, \omega_{SC}\}^T$, while $u \in \mathbb{R}^3$ is the control input, $d^u \in \mathbb{R}^3$ is the input disturbances, and $d^y \in \mathbb{R}^3$ is the sensor uncertainties. This model is discretized via the forward Euler method, leading to

$$\begin{cases} x_{k+1} &= F_k x_k + G u_k + d_k \\ y_k &= C x_k + d_k^y \end{cases}, \tag{15}$$

where F_k, G and d_k are respectively defined as

$$\begin{cases} F_k &= I + \tau A(x_k) \\ G &= \tau B \\ d_k &= \tau B d_k^u \end{cases}. \tag{16}$$

The EKF algorithm is based on two main steps: *Prediction* and *Update*. At each time step k, the predicted state x_k^p and predicted covariance matrix P_k^p of the estimation error are computed as

$$\begin{cases} x_k^p &= F_k \hat{x}_{k-1} + G u_{k-1} \\ P_k^p &= F_{k-1} P_{k-1} F_{k-1}^\top + Q^d \end{cases}. \tag{17}$$

Then, using the measurement y_k coming from the sensor, the estimated state $\hat{x}_k$ and P_k are updated according to

$$\begin{cases} S_k &= C P_k^p C^\top + R^d \\ K_k &= P_k^p C^\top S_k^{-1} \\ \Delta y_k &= y_k - C x_k^p \\ \hat{x}_k &= x_k^p + K_k \Delta y_k \\ P_k &= (I - K_k C) P_k^p \end{cases}, \tag{18}$$

where Q^d and R^d are matrices that can be suitably tuned, representing respectively the covariance of the input disturbance d_k and the covariance of the measurement process d_k^y. Such an EKF is used to filter out the noise from the spacecraft measurements provided by CAS and STR, in order to improve the anti-windup performance.

ACKNOWLEDGMENT

This work was funded by the European Space Agency. The Authors ensure complete objectivity in the data interpretation and writing of the paper. The view expressed in this work cannot be taken as the official position of the European Space Agency.

REFERENCES

[1] P. Amaro-Seoane, H. Audley, S. Babak, J. Baker, E. Barausse, P. Bender, E. Berti, P. Binetruy, M. Born, D. Bortoluzzi, *et al.*, "Laser interferometer space antenna," *arXiv preprint arXiv:1702.00786*, 2017.

[2] K. Danzmann, T. Prince, P. Binetruy, *et al.*, "ESA LISA Yellow Book," 2011.

[3] S. Vidano, C. Novara, J. Grzymisch, and M. Pagone, "The LISA DFACS: Overview of the control design activities for the drag-free mode," in *11th ESA Guidance Navigation and Control Conference*, 2021.

[4] C. Novara *et al.*, "Assessment and preliminary prototyping of a drag free control system for the L3 gravity wave observatory." 2020.

[5] J. Thorpe, T. Littenberg, J. Baker, J. Slutsky, *et al.*, "Lisa pathfinder as a micrometeoroid instrument," in *Journal of Physics: Conference Series*, vol. 840, no. 1. IOP Publishing, 2017, p. 012007.

[6] J. I. Thorpe, J. Slutsky, J. G. Baker, T. B. Littenberg, S. Hourihane, N. Pagane, P. Pokorny, D. Janches, M. Armano, H. Audley, *et al.*, "Micrometeoroid events in lisa pathfinder," *The Astrophysical Journal*, vol. 883, no. 1, p. 53, 2019.

[7] M. Virdis, S. Vidano, M. Pagone, D. Ruggiero, C. Novara, J. Grzymisch, V. Preda, and E. Punta, "The LISA DFACS: effects of micrometeoroid impacts in the drag-free mode," in *IAC Conference*, 2021.

[8] J. C. Doyle, R. S. Smith, and D. F. Enns, "Control of plants with input saturation nonlinearities," in *1987 American Control Conference*, 1987, pp. 1034–1039.

[9] I. Salgado, I. Chairez, J. Moreno, L. Fridman, and A. Poznyak, "Generalized super-twisting observer for nonlinear systems," *IFAC Proceedings Volumes*, vol. 44, no. 1, pp. 14 353–14 358, 2011, 18th IFAC World Congress.

[10] R. Martinez-Guerra and J. Mata-Machuca, *Fault estimation using sliding mode observers*. Springer, 2014.

[11] M. Hussain, M. Rehan, S. Ahmed, T. Abbas, and M. Tufail, "A novel approach for static anti-windup compensation of one-sided lipschitz systems under input saturation," *Applied Mathematics and Computation*, vol. 380, p. 125229, 2020.

[12] S. Tarbouriech and M. Turner, "Anti-windup synthesis: An overview of some recent advances and open problems. iet control theory appl. 3(1), 1-19," *Control Theory & Applications, IET*, vol. 3, pp. 1 – 19, 02 2009.

[13] F. Wu and B. Lu, "Anti-windup control design for exponentially unstable lti systems with actuator saturation," *Systems & Control Letters - SYST CONTROL LETT*, vol. 52, pp. 305–322, 07 2004.

[14] G. Ellis, "Chapter 18 - using the luenberger observer in motion control," in *Control System Design Guide (Fourth Edition)*, G. Ellis, Ed. Boston: Butterworth-Heinemann, 2012, pp. 407–429.

[15] X. yan Yu and L. Chen, "Modeling and observer-based augmented adaptive control of flexible-joint free-floating space manipulators," *Acta Astronautica*, vol. 108, pp. 146–155, 2015.

[16] G. Welch, G. Bishop, *et al.*, "An introduction to the kalman filter," 1995.

[17] K. Fujii, "Extended kalman filter," *Refernce Manual*, pp. 14–22, 2013.

[18] S. K. Spurgeon, "Sliding mode observers - historical background and basic introduction," 2015.

[19] Y. Hu, P. Huang, Z. Meng, D. Wang, and Y. Lu, "Approaching control for tethered space robot based on disturbance observer using super twisting law," *Advances in Space Research*, vol. 61, no. 9, pp. 2344–2351, 2018.

[20] Y.-C. Liu, S. Laghrouche, D. Depernet, A. Djerdir, and M. Cirrincione, "Disturbance-observer-based complementary sliding-mode speed control for pmsm drives: A super-twisting sliding-mode observer-based approach," *IEEE Journal of Emerging and Selected Topics in Power Electronics*, vol. 9, no. 5, pp. 5416–5428, 2020.

[21] F. Piltan and J.-M. Kim, "Bearing fault diagnosis by a robust higher-order super-twisting sliding mode observer," *Sensors*, vol. 18, no. 4, p. 1128, 2018.

[22] S. Vidano, C. Novara, L. Colangelo, and J. Grzymisch, "The LISA DFACS: A nonlinear model for the spacecraft dynamics," *Aerospace Science and Technology*, vol. 107, p. 106313, 2020.

[23] A. Levant, "Robust exact differentiation via sliding mode technique," *Automatica*, vol. 34, no. 3, pp. 379–384, 1998.

[24] J. Picó, E. Picó-Marco, A. Vignoni, and H. De Battista, "Stability preserving maps for finite-time convergence: Super-twisting sliding-mode algorithm," *Automatica*, vol. 49, no. 2, pp. 534–539, 2013.